High color purity phosphors of $LaAlGe_2O_7$ doped with Tm^{3+} and Er^{3+}

Yu-Chun Li, Yen-Hwei Chang,[a] Yu-Feng Lin, and Yi-Jing Lin
Department of Materials Science and Engineering, National Cheng Kung University, Tainan 70101, Taiwan

Yee-Shin Chang
Institute of Electro-Optical and Materials Science, National Formosa University, Huwei, Yunlin 632, Taiwan

(Received 8 March 2006; accepted 29 June 2006; published online 23 August 2006)

Phosphors of $LaAlGe_2O_7$ doped with Tm^{3+} and Er^{3+} of high color purity, exhibiting a narrow band emission in the blue and green regions, were obtained. $(La_{1-x}Ln_x)AlGe_2O_7$ (Ln=Tm,Er) powders are bright emitters, with chromaticity color coordinates that are comparable to or better than those of standard phosphors for display or lighting devices. The blue emission of the Tm^{3+}-doped phosphor had CIE chromaticity coordinates (0.151, 0.033) with a dominant wavelength of 455 nm and a color purity of 94%. The Er^{3+}-doped phosphor had color coordinates (0.249, 0.718), a dominant wavelength of 542 nm, and 92% purity. © *2006 American Institute of Physics*.
[DOI: 10.1063/1.2337275]

Rare-earth-ion-doped crystallite has attracted considerable research interest owing to its excellent luminescent properties.[1] The use of rare-earth element-based phosphor, based on "line-type" *f-f* transitions, can narrow the emissions to the visible range, resulting in high efficiency and a high lumen equivalent. Thulium-doped phosphors have attracted substantial attention in recent years because Tm^{3+} ions provide blue luminescence with potential applications in screens and displays, such as cathode-ray tube screens, field-emission displays, and electroluminescent devices.[2–4] Conventional blue phosphors (ZnS: Ag, ZnS: Tm, F) are the most efficient blue light emitters.[5,6] However, using sulfide-based materials has such disadvantages as chemical instability during operation, corrosion of the emitter cathode in field-emission displays induced by sulfur-related contaminant gases,[7] and luminance saturation at high excitation density.[8] Hence, the use of oxide-based phosphors as a source of radiation is an emerging field. Certainly, oxides such as Y_2O_3: Tm, $SrHfO_3$: Tm, and Y_3GaO_6: Tm are serviceable alternatives to the presently used sulfides.[2,8,9]

Erbium-doped materials have been widely adopted in optical telecommunications systems because of their particular emission band around 1.53 μm in the IR region.[10] More recently, however, Er-activated materials have been studied as a light source because of their green emissions.[11,12] In this study, $LaAlGe_2O_7$ activated with Tm^{3+} and Er^{3+} was prepared, and its photoluminescence (PL) characteristics were investigated.

Tm^{3+}- and Er^{3+}-doped $LaAlGe_2O_7$ were synthesized by a vibrating milled solid state reaction. The starting materials were La_2O_3, GeO_2, Al_2O_3, Tm_2O_3, and Er_2O_3. After they had been mechanically activated by grinding in a high energy vibromill, the mixtures were calcined at 1250 °C in air for 12 h. Conventional x-ray diffraction technique was employed to identify the phase. The data of all the samples reveal a single phase without any impurity and indicate that the Tm^{3+} and Er^{3+} ions were satisfactorily substituted for the La^{3+} ions.

[a]Author to whom correspondence should be addressed; FAX: +886-6-2382800; electronic mail: enphei@mail.ncku.edu.tw

Figure 1 presents PL excitation and emission spectra associated with Tm^{3+} ions in $LaAlGe_2O_7$. The sharp excitation peaks between 200 and 400 nm are assigned to the typical $4f^n \rightarrow 4f^n$ intraconfiguration forbidden transitions of Tm^{3+}. Tm^{3+} has complicated energy levels and various possible transitions because of a strong deviation from *R-S* coupling in the 4*f* configuration. Accordingly, the excited states of Tm^{3+} ions may relax via a large number of paths, giving rise to ultraviolet, visible, and infrared emission with moderate intensity.[13] The major emission peak of Tm^{3+} was at 453 nm and a very weak peak was observed at 512 nm, corresponding to the transitions $^1D_2 \rightarrow {}^3F_4$ and $^1D_2 \rightarrow {}^3H_5$, respectively. Compared to conventional Tm-doped phosphors, particularly noteworthy is that the transitions from $^1G_4$ to ^3H_J manifold do not appear in $LaAlGe_2O_7$, such as $^1G_4 \rightarrow {}^3H_6$ (~475 nm). Reisfeld[14] has noted that nonradiative relaxation between various *J* states of rare-earth ions may occur by the simultaneous emission of several phonons which conserve

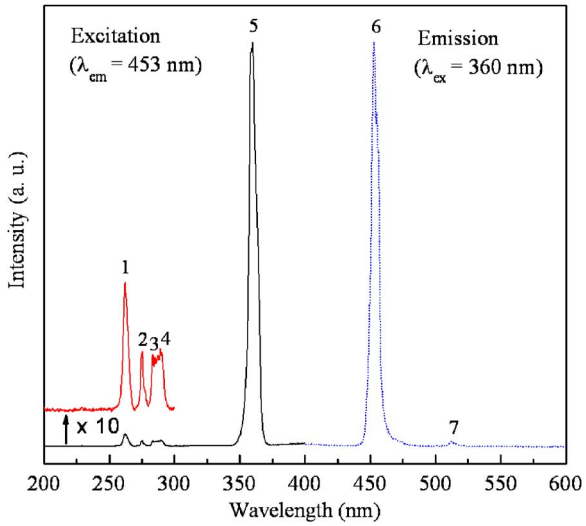

FIG. 1. (Color online) PL excitation and emission spectra of $LaAlGe_2O_7$: Tm phosphor measured at room temperature. The excitation peaks depicted from 1 to 5 are assigned to transitions between the ground $^3H_6$ level and the excited $^3P_2$, $^3P_1$, $^3P_0$, $^1I_6$, and $^1D_2$ levels, respectively. The emission peaks depicted from 6 to 7 correspond to the $^1D_2 \rightarrow {}^3F_4$ and $^1D_2 \rightarrow {}^3H_5$ transitions, respectively.

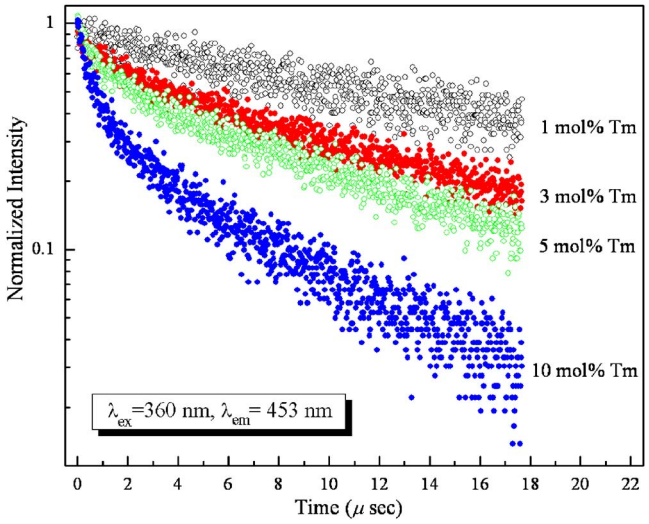

FIG. 2. (Color online) Decay curves of $^1D_2 \rightarrow {}^3F_4$ emission for various Tm^{3+} concentrations in $LaAlGe_2O_7$ under excitation at 360 nm. The signals were detected at 453 nm.

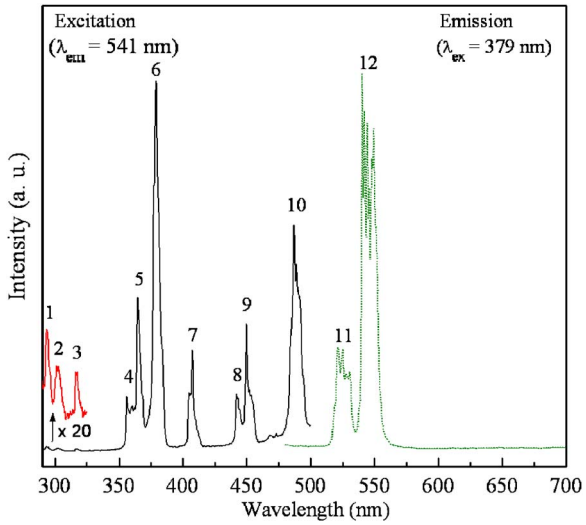

FIG. 3. (Color online) PL excitation and emission spectra of $LaAlGe_2O_7$: Er phosphor measured at room temperature. The excitation peaks depicted from 1 to 10 are assigned to transitions between the ground $^4I_{15/2}$ level and the excited $^4G_{7/2}$, $^2K_{13/2}$, $^2P_{3/2}$, $^2G_{7/2}$, $^4G_{9/2}$, $^4G_{11/2}$, $^2H_{9/2}$, $^4F_{3/2}$, $^4F_{5/2}$, and $^4F_{7/2}$ levels, respectively. The emission peaks depicted from 11 to 12 are attributed to the $^2H_{11/2} \rightarrow {}^4I_{15/2}$ and $^4S_{3/2} \rightarrow {}^4I_{15/2}$ transitions, respectively.

the energy of the transitions, and these multiphonon processes arise from the interaction of the electronic levels of the rare earth with the vibrations of the host lattice. Therefore, it may be expected that very efficient nonradiative relaxation for the $^1G_4$ level would occur in $LaAlGe_2O_7$ lattice. The blue $^1D_2 \rightarrow {}^3F_4$ emission is quite sharp, with a full width at half maximum of about 6 nm. This spectral feature reveals high color purity and excellent chromaticity coordinate characteristics. A series of $La_{1-x}Tm_xAlGe_2O_7$ samples was synthesized as the dopant concentration ranged from 0.1 to 30 mol %. The most efficient PL intensities occurred at $x=0.03$ in the $(La_{1-x}Tm_x)AlGe_2O_7$ system. The drop in intensity as the Tm^{3+} content increased (concentration quenching effect) was caused by the rise of nonradiative decay channels, which was promoted by the interaction with quenching centers during the cross relaxation or energy transfer processes among Tm^{3+} ions.

The effect of Tm^{3+} content on the $^1D_2 \rightarrow {}^3F_4$ transition decay curves is shown in Fig. 2. A single exponential decay was observed in the diluted samples. At higher concentrations, however, the observed decay curves were nonexponential, and the nonexponential change becomes more prominent as Tm^{3+} content increases, revealing that more than one relaxation process exists. When the luminescent centers have different local environments, the associated ions will relax at different rates. If the rates are dramatically different, then diverse decay curves are likely to be observed. Nevertheless, the low-doped samples yield single exponential decay curves with a long lifetime, eliminating this possibility. Additionally, it is unlikely that only one site with the shorter lifetime is populated for higher concentration. The energy transfer over ion-ion interaction between two neighboring activator ions would be beneficial to resolve this issue. The distance between Tm^{3+} ions decreases as the Tm^{3+} concentration increases; subsequently, the energy transfer process between Tm^{3+} ions becomes more frequent, providing an extra decay channel which changes the decay curves.

Samples with low Tm^{3+} content would minimize the effects of the interactions between optically active ions. The monoexponential decay curve fit indicates that the $LaAlGe_2O_7$ contains a unique crystallographic site available for the activator (Tm^{3+} instead La^{3+}), so that only one luminescent mechanism applies. This result is inconsistent with preliminary investigations of the $LnAlGe_2O_7$-type (Ln: trivalent rare-earth ions) structure, where Ln^{3+} ions are incorporated into single-centered hosts until all rare-earth sites have been substituted.[15]

Trivalent erbium with the $4f^{11}$ configuration has complex energy levels with various possible transitions between $4f$ levels. The transitions between these $4f$ levels are highly selective and are associated with sharp lines in the spectra. Figure 3 shows PL excitation and emission spectra of $LaAlGe_2O_7$: Er. The excitation spectrum consists of a series of sharp intra-$4f$-shell transitions from the ground state $^4I_{15/2}$ to higher energy levels. For all samples, only green emission was observed and attributed to the transition from the $^2H_{11/2}$ and $^4S_{3/2}$ states to the $^4I_{15/2}$ ground state. In particular, the emission peaks were centered in the green region, so its color coordinates were desirable. Such partial emission in only the green region with favorable color coordinates is unusual for Er^{3+} than other inorganic oxide host,[16] where emission is observed between 500 and 700 nm with moderate intensity. Red emission assigned to the $^4F_{9/2} \rightarrow {}^4I_{15/2}$ ($\sim$660 nm) transition for Er^{3+} was not detected, indicating that a very efficient nonradiative relaxation for the $^4F_{9/2}$ level occurred. The dependence of the Er^{3+} decay curves on concentration is analogous to that of the decay curves of Tm^{3+}. The former deviated from the single exponential as the concentration of Er^{3+} ions increased.

The corresponding chromaticity Commission International de l'Eclairage (CIE) coordinates are illustrated in Fig. 4. With the (x,y) chromaticity coordinates, the dominant wavelength and the color purity compared to CIE Standard Source C [illuminant C=(0.3101,0.3162)] for Tm^{3+}- and Er^{3+}-doped phosphors are listed in Table I. For Tm-doped $LaAlGe_2O_7$, the values obtained (0.151, 0.033), with a color purity of 94%, are superior (high color purity) to those reported for currently available commercial blue phosphors, such as Y_2O_3: Tm (0.158, 0.150),[2] $Sr_2B_5O_9Cl$: Tm (0.166,

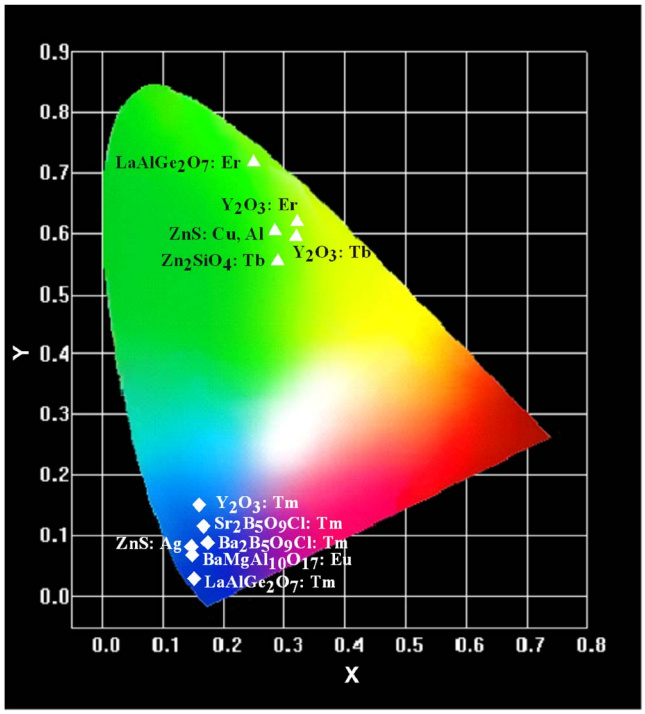

FIG. 4. (Color online) CIE chromaticity diagram showing the color coordinates of Tm- and Er-doped $LaAlGe_2O_7$ phosphors and standard blue and green emitters.

0.115),[17] $Ba_2B_5O_9Cl$: Tm (0.172, 0.088),[18] ZnS: Ag (0.145, 0.081),[19] and $BaMgAl_{10}O_{17}$: Eu (0.147, 0.067).[20] In comparison with green phosphors Y_2O_3: Tb (0.319, 0.597),[2] Zn_2SiO_4: Tb (0.287, 0.554),[21] ZnS: Cu, Al (0.284, 0.605),[22] and Y_2O_3: Er (0.32, 0.62),[12] the Er-doped $LaAlGe_2O_7$ had preferable CIE (0.249, 0.718) and color purity (92%). These information provide evidence that the Tm^{3+}- and Er^{3+}-doped $LaAlGe_2O_7$ phosphors exhibit vivid blue and green emissions with CIE color coordinates and color purity that are comparable to or better than those reported for the most-used phosphors. Furthermore, the Tm^{3+} and Er^{3+} phosphors allow a wide color gamut that is much wider than that recommended by the European Broadcasting Union (EBU) and the National Television System Committee (NTSC) primary system colors [EBU illuminant blue=(0.15,0.06), green =(0.29,0.60); NTSC illuminant blue=(0.14,0.08), green =(0.21,0.71)]. Phosphors with such high color purity emit primarily blue and green, from which a wide spectrum of colors is generated by appropriate mixing.

TABLE I. Chromaticity coordinate, dominant wavelength, and color purity for blue and green phosphors.

Phosphor	CIE (x,y)	Dominant wavelength (nm)	Purity (%)
$LaAlGe_2O_7$:Tm	(0.151, 0.033)	455	94
$LaAlGe_2O_7$:Er	(0.249, 0.718)	542	92

In summary, the emission spectra of the Tm^{3+}- and Er^{3+}-doped $LaAlGe_2O_7$ samples corresponded to vivid blue and green emissions. The presence of a single optically active site in $LaAlGe_2O_7$ may explain the monoexponential decay curves for samples with low activator concentrations, where the energy transfer between activator ions is negligible. The lanthanide germinates in the system $(La_{1-x}Ln_x)AlGe_2O_7$ (Ln=Tm,Er) samples clearly exhibit excellent chromaticity coordinates of (0.151, 0.033) with a color purity of 94% and (0.249, 0.718) with a color purity of 92% when doped with Tm and Er, respectively.

The authors would like to thank the National Science Council of Taiwan, Republic of China, for financially supporting this research under Contract No. NSC94-2216-E-006-017.

[1] C. Feldmann, T. Justel, C. R. Ronda, and P. J. Schmidt, Adv. Funct. Mater. **13**, 511 (2003).
[2] J. Hao, S. A. Studenikin, and M. Cocivera, J. Lumin. **93**, 313 (2001).
[3] Y. Nakanishi, H. Wada, H. Kominami, M. Kottaisamy, T. Aokib, and Y. Hatanaka, J. Electrochem. Soc. **146**, 4320 (1999).
[4] J. H. Kim, M. R. Davidson, and P. H. Holloway, Appl. Phys. Lett. **83**, 4746 (2003).
[5] M. Ollinger, V. Craciun, and K. Singh, Appl. Phys. Lett. **80**, 1927 (2002).
[6] S. H. Sohn and Y. Hamakawa, Appl. Phys. Lett. **62**, 2242 (1993).
[7] O. A. Lopez, J. McKittric, and L. E. Shea, J. Lumin. **71**, 1 (1997).
[8] H. Yamamoto, M. Mikami, Y. Shimomura, and Y. Oguri, J. Lumin. **87-89**, 1079 (2000).
[9] F. S. Liu, B. J. Sun, J. K. Liang, Q. L. Liu, J. Luo, Y. Zhang, L. X. Wang, J. N. Yao, and G. H. Rao, J. Solid State Chem. **78**, 1064 (2005).
[10] J. Wu, P. Punchaipetch, R. M. Wallace, and J. L. Coffer, Adv. Mater. (Weinheim, Ger.) **16**, 1444 (2004).
[11] A. J. Steckl, J. Heikenfeld, D. S. Lee, and M. Garter, Mater. Sci. Eng., B **81**, 97 (2001).
[12] Y. Nakanishi, K. Kimura, H. Kominami, H. Nakajima, Y. Hatanaka, and G. Shimaoka, Appl. Surf. Sci. **212-213**, 815 (2003).
[13] G. Qin, W. Qin, C. Wu, S. Huang, J. Zhang, S. Lu, D. Zhao, and H. Liu, J. Appl. Phys. **93**, 4328 (2003).
[14] R. Reisfeld, *Structure and Bonding* (Springer, New York, 1975), Vol. 22, pp. 123–175.
[15] A. A. Kaminskii, B. V. Mill, A. V. Butashin, E. L. Belokoneva, and K. Kurbanov, Phys. Status Solidi A **103**, 575 (1987).
[16] F. Vetrone, J. C. Boyer, J. A. Capobianco, A. Speghini, and M. Bettinelli, Chem. Mater. **15**, 2737 (2003).
[17] J. Hao and M. Cocivera, J. Phys.: Condens. Matter **14**, 925 (2002).
[18] J. Hao, J. Gao, and M. Cocivera, Appl. Phys. Lett. **82**, 2224 (2003).
[19] T.L Jüstel, H. Nikol, and C. R. Ronda, Angew. Chem., Int. Ed. **37**, 3085 (1998).
[20] C. R. Ronda, J. Lumin. **72-74**, 49 (1997).
[21] H. X. Zhang, S. Buddhudu, C. H. Kam, Y. Zhou, Y. L. Lam, K. S. Wong, B. S. Ooi, S. L. Ng, and W. X. Que, Mater. Chem. Phys. **68**, 31 (2001).
[22] C. H. Chang, B. S. Chiou, K. S. Chen, C. C. Ho, and J. C. Ha, Ceram. Int. **31**, 635 (2005).